ISSN (Online) 2456 -1304

International Journal of Science, Engineering and Management (IJSEM)

Volume 13, Issue 9, September 2026

Activated Carbon Decorated Polypyrrole–Chitosan/Zinc Oxide Bio-Composite Derived from Shrimp Shell and Rice Husk for Enhanced Methylene Blue Adsorption and Antibacterial Applications

[1] Lubna S. Majgaonkar*, [2] Dr. Rupinder Kaur, [3] Dr. Surajit Some

[1] G.N. Khalsa College, Matunga, Mumbai, Maharashtra, India
[2] Professor, G.N. Khalsa College, Mumbai, Maharashtra, India
[3] UGC Assistant Professor, Department of Specialty Chemicals Technology (ICT), Mumbai, Maharashtra, India
*Corresponding Author Email: [1] lubna.siraj@gnkhalsa.edu.in

Abstract*— The Shrimp shell and rice husk wastes were transformed via a one-pot synthesis into a sustainable AC/CH/ZnO/PPy bio-composite with a porous, conductive structure, enhanced surface functionality, improved mechanical stability, and abundant active sites for wastewater treatment. The Comprehensive characterization by FTIR, SEM, TEM and XRD, confirmed successful composite formation, crystalline ZnO incorporation, and increased surface area and porosity. Batch adsorption tests confirmed the functionality of the novel bio-composite, achieving 97.21% removal at pH 7.5 and 97.32% removal at 150 ppm after 50 min, with optimum conditions of 25 mg adsorbent dosage and 35 min contact time. The adsorption kinetics followed the pseudo-second-order model, indicating that adsorption was governed by the availability of active sites and adsorbate uptake. The composite demonstrated antibacterial activity, with inhibition zones of 13 mm against E. coli and 14 mm against S. aureus, indicating its potential for dual-function wastewater remediation. Overall, this eco-friendly, low cost, and scalable approach converts agricultural and seafood wastes into a high-performance material for dye contaminated wastewater remediation and related environmental and antibacterial applications.

Keywords: Activated carbon, Chitosan, Polypyrrole, Zinc oxide nanoparticles, Methylene blue, Adsorption.

I. INTRODUCTION

The Water pollution caused by untreated industrial, agricultural, and domestic wastewater is a major global concern, with serious impacts on aquatic ecosystems and human well-being [1]. The Synthetic dyes discharged from textile, paper, leather, pharmaceutical, and chemical industries are particularly problematic because of their intense colour, chemical stability, persistence, and low biodegradability; they can reduce light penetration, inhibit photosynthesis, disturb aquatic ecosystems, and pose toxic risks to humans and aquatic organisms [1,2]. Methylene blue (MB), a widely used cationic dye, is frequently employed as a model pollutant because of its water solubility, stability, and resistance to degradation [3]. Conventional treatment methods may involve high costs, operational complexity, incomplete removal, or secondary pollution, whereas adsorption provides a simple and economical alternative [3,4]. Renewable biomass and industrial wastes are increasingly explored as sustainable adsorbent resources; rice-husk-derived activated carbon provides a porous framework, while chitosan-based materials offer functional groups that facilitate MB binding [4,5]. In this study, an activated carbon/chitosan/zinc oxide/polypyrrole (AC/CH/ZnO/PPy) bio-composite was developed for MB removal, integrating adsorption with photocatalytic degradation and enhanced charge separation through PPy–ZnO interaction [6].

II. MATERIALS AND METHODOLOGY

A. Materials

- Shrimp shell waste was collected from local seafood markets and rice husk was obtained from nearby granary. Pyrrole monomer, ferric chloride ($FeCl_3$), zinc chloride ($ZnCl_2$), concentrated sulphuric acid (H_2SO_4), sodium hydroxide (NaOH), and distilled water were used for synthesis of the bio-composite. All chemicals used in the study were of analytical grade.

B. Chemicals and Reagents:

- All chemicals used in this study were of analytical reagent (AR) grade and were used without further purification. Pyrrole monomer (99%) and methylene blue (MB) were procured from Sigma-Aldrich**,** while ferric chloride ($FeCl_3$)**,** zinc chloride ($ZnCl_2$)**,** sodium hydroxide (NaOH) pellets**,** and concentrated sulphuric acid (H_2SO_4) were obtained from Merck**.** Distilled water was used for the preparation of all solutions throughout the study.

ISSN (Online) 2456 -1304

International Journal of Science, Engineering and Management (IJSEM)

Volume 13, Issue 9, September 2026

C. Preparation of Activated Carbon Decorated Polypyrrole–Chitosan/Zinc Oxide Bio-composite (AC/CH/ZnO/PPy):

The Shrimp shells were washed, dried at 60 °C for 24 h, ground, and sieved. The resulting powder (3 g) was treated with 50 mL concentrated H_2SO_4 for 2 h under continuous stirring. Rice husk (3 g) and an additional 35 mL concentrated H_2SO_4 were then added to promote carbonization and activation. After cooling the mixture to 0–5 °C, pyrrole (2 mL) and $FeCl_3$ (5 mL, 1 M) were added gradually, and oxidative polymerization proceeded for 16 h. The product was filtered through Whatman No. 1 paper, washed, and dispersed in 400 mL $ZnCl_2$ (0.2 M). Subsequently, 125 mL NaOH (13 M) was added, and the mixture was stirred for 4 h at 4–5 °C to facilitate ZnO formation and chitin deacetylation. The AC/CH/ZnO/PPy bio-composite was filtered, washed to neutral pH, dried overnight at 60 °C, and stored in airtight containers.

D. Characterization of the Synthesized Bio-Composite:

The synthesized activated carbon/chitosan/zinc oxide/polypyrrole (AC/CS/ZnO/PPy) bio-composite was characterized using FTIR, SEM, TEM, XRD, and UV–Vis spectroscopy. The FTIR analysis identified the functional groups and chemical interactions within the composite. SEM and TEM were used to examine surface morphology, particle distribution, and porous structure. The XRD analysis determined the crystalline structure, phase composition, and incorporation of ZnO nanoparticles. UV–Vis spectroscopy evaluated methylene blue adsorption by measuring the residual dye concentration at its maximum absorption wavelength (λmax=664 nm). These analyses confirmed the composite's structural, morphological, crystalline, and optical characteristics.

E. Batch Adsorption Studies:

- The Batch adsorption experiments were conducted using methylene blue dye solutions under varying experimental conditions, including solution pH, contact time, adsorbent dosage, and initial dye concentration.
- The percentage dye removal was calculated using the formula:

$$\%\ Removal = \frac{C_0 - C_e}{C_0} \times 100$$

Where:
C_0= Initial dye concentration
C_e= Equilibrium dye concentration

F. Adsorption Kinetics:

The adsorption kinetics of methylene blue (MB) onto the synthesized bio-composite were investigated using dye solutions with initial concentrations of 50, 75, 100, 125, 150, 175 mg/L**.** For each experiment, 50 mg of the bio-composite was added to 50 mL of MB solution. Samples were collected at 5-min intervals up to 60 min. At each interval, the adsorbent was separated by filtration, and the residual MB concentration in the filtrate was determined using a UV–visible spectrophotometer. The adsorption capacity at time t *(q_t)* was calculated using:

$$q_t = \frac{(C_0 - \dot{C}_t)}{m} v$$

- where C_0 and C_t are the initial and residual MB concentrations (mg L^{-1}), respectively, V is the solution volume (L), and m is the mass of the adsorbent (g). The experimental kinetic data were fitted using the pseudo-first-order and pseudo-second-order models, which are commonly applied to evaluate adsorption-rate behaviour.
- The pseudo-first-order kinetic model is expressed as:

$$\mathrm{I_n}(qe - qt) = \mathrm{In}q_e - kt$$

where qe (mg g^{-1}) is the equilibrium adsorption capacity, qt (mg g^{-1}) is the adsorption capacity at time *t*, and k_1 (min^{-1}) is the pseudo-first-order rate constant.

The pseudo-second-order kinetic model is represented by:

$$\frac{t}{qt} = \frac{1}{k_2 q_e^2} + \frac{t}{q_e}$$

where q_t= amount of dye adsorbed at time t(mg/g), q_e= adsorption capacity at equilibrium (mg/g), k_2 = pseudo-second-order rate constant $(g\, mg^{-1}\, min^{-1})$ t = contact time (min).

The kinetic parameters were obtained from the linear plots of the respective equations, and the applicability of each model was evaluated based on the correlation coefficient (R^2) and the agreement between the calculated and experimental equilibrium adsorption capacities.

G. Antibacterial Activity:

The antibacterial activity of the AC/CS/ZnO/PPy bio-composite was evaluated against Gram-positive *Staphylococcus aureus* and Gram-negative *Escherichia coli* using the agar well diffusion method. Fresh cultures were grown in Mueller–Hinton broth for 24 h and adjusted to 0.5 McFarland standard (approximately 1 × 10^8 CFU/mL), followed by dilution to 1 × 10^6 CFU/mL. The bacterial suspensions were uniformly spread on Mueller–Hinton agar plates, and sterile wells were loaded with 100 µL of the bio-composite suspension. The Chloramphenicol and sterile distilled water served as positive and negative controls, respectively. The plates were incubated at 37 °C for 24 h, after which antibacterial activity was assessed by measuring the inhibition zones around the wells. The efficacy of the bio-composite was determined by comparing its inhibition zones with those of the controls.

ISSN (Online) 2456 -1304

International Journal of Science, Engineering and Management (IJSEM)

Volume 13, Issue 9, September 2026

III. RESULTS AND DISCUSSION

A. Characterization of AC/CH/ZnO/PPy Bio-composite

Fourier Transform Infrared Spectroscopy (FTIR):

FTIR analysis confirmed the characteristic functional groups of the AC/CH/ZnO/PPy bio-composite. The broad band at 3350.31 cm^{-1} corresponded to O–H and N–H stretching vibrations of chitosan. The band at 1590.25 cm^{-1} was attributed to C=C stretching of polypyrrole with possible contribution from chitosan amide vibrations, while 1399.98 cm^{-1} represented C–N stretching/N–H deformation. The bands at 1041.28 and 971.07 cm^{-1} were associated with C–O and polysaccharide vibrations. The band at 872.56 cm^{-1} indicated aromatic C–H bending, whereas 451.31 and 410.68 cm^{-1} corresponded to Zn–O lattice vibrations, confirming ZnO incorporation [7–9]. Overall, the spectrum confirmed integration of activated carbon, chitosan, polypyrrole, and ZnO through hydroxyl, amino, nitrogen-, and oxygen-containing functionalities. These groups provide potential sites for methylene blue interaction, while chitosan and polypyrrole functionalities may facilitate dye–adsorbent interactions [8,10].

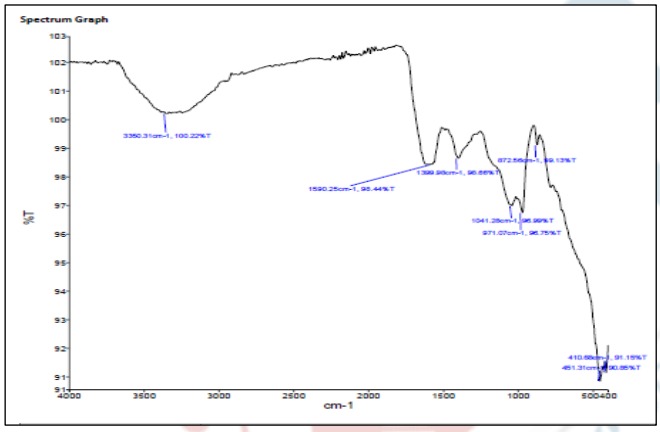


Figure 1. FTIR – (AC/CH/ZnO/PPy) Bio-composite

Scanning Electron Microscopy (SEM) and Transmission Electron Microscopy (TEM):

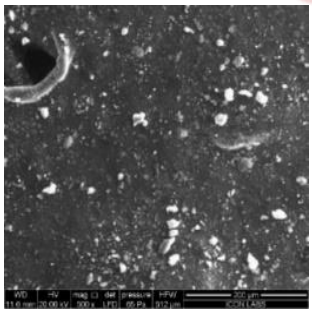


Fig. 2.a

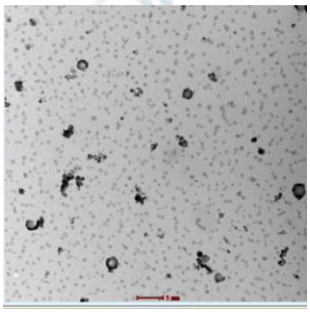


Fig. 2.b

Fig.2. (a). SEM image and (b). TEM image of synthesized AC/CH/ZnO/PPy bio-composite

SEM analysis revealed spherical to granular ZnO nanoparticles with localized agglomeration, along with interconnected porous, fibrous, and flaky structures associated with the chitosan/polypyrrole-containing matrix [7,9]. The rough and porous morphology may enhance surface accessibility and dye diffusion, supporting methylene blue adsorption, while ZnO incorporation may provide additional antibacterial functionality [7,9].

TEM analysis showed predominantly quasi-spherical particles with broad size distribution and localized aggregation. Individual particles and overlapping darker regions were observed, with aggregation potentially arising from interparticle interactions and sample preparation [9,11]. Based on the 1 µm scale bar, features ranged from nanometre to sub-micrometre scales. Quantitative image analysis would be required for reliable particle-size determination. Overall, TEM confirmed the particle morphology, dispersion, and localized aggregation of the AC/CH/ZnO/PPy bio-composite.

X-Ray Diffraction (XRD):

The XRD analysis confirmed the crystalline phase and successful incorporation of ZnO nanoparticles into the AC/CH/PPy matrix. Characteristic peaks at 31.8°, 34.4°, 36.2°, 47.5°, 56.6°, and 62.8°, indexed to the (100), (002), (101), (102), (110), and (103) planes, respectively, confirmed the hexagonal crystalline structure of ZnO. The broad peak at 20–25° indicated amorphous carbon and partially crystalline chitosan/polypyrrole phases. Peak broadening suggested nanoscale ZnO crystallites, supporting the SEM and FTIR findings.

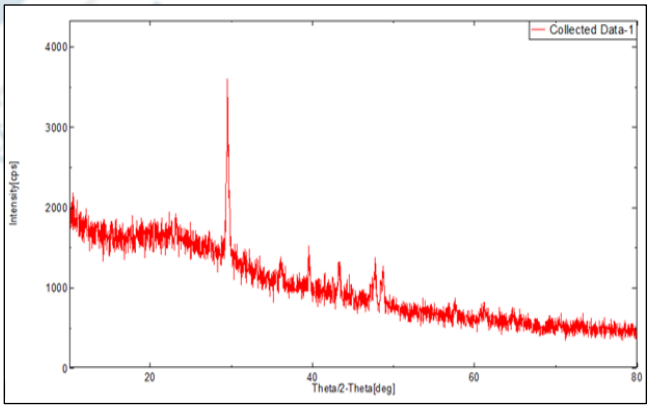


Fig. 3. XRD pattern of synthesized AC/CH/ZnO/PPy bio-composite showing characteristic diffraction peaks.

B. Effect of Adsorption Parameters

Effect of pH:

The solution pH significantly affected methylene blue adsorption by the AC/CH/ZnO/PPy bio-composite. The adsorption capacity increased from 105.5 mg/g at pH 6 to 243.03 mg/g at pH 7.5, while removal efficiency increased from 42.2% to 97.21%. This enhancement can be attributed to reduced competition from H^+ ions and increased electrostatic attraction between the negatively charged adsorbent surface and cationic methylene blue molecules. At

ISSN (Online) 2456 -1304

International Journal of Science, Engineering and Management (IJSEM)

Volume 13, Issue 9, September 2026

pH 8.5, adsorption slightly decreased to 226.77 mg/g, with a removal efficiency of 90.67%. Therefore, pH 7.5 provided the optimum conditions for methylene blue adsorption under the studied conditions.

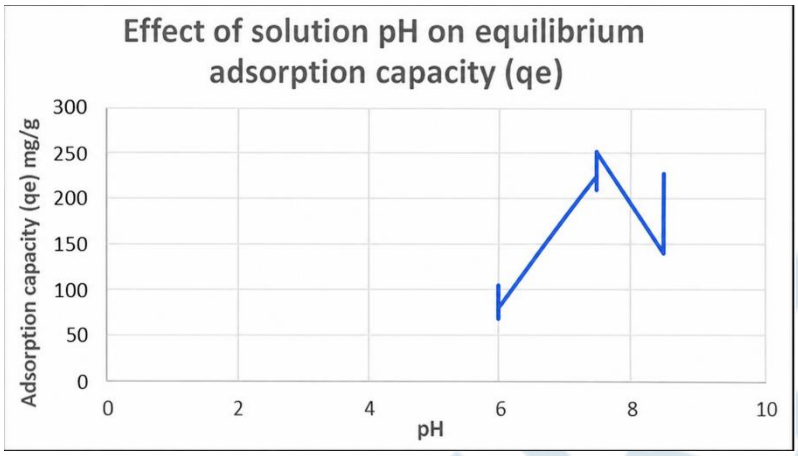


Fig. 4. Effect of pH on Methylene Blue Removal Efficiency

Table 1. Effect of solution pH on methylene blue adsorption capacity and removal efficiency

pH condition	pH	Initial MB concentration (C_0) (mg/L)	Equilibrium concentration (C_e) (mg/L)	Equilibrium adsorption capacity(q_e)(mg/g)	Removal efficiency (%)
Acidic	6	25	14.45	105.5	42.2
Neutral	7.5	25	0.67	243.03	97.21
Basic	8.5	25	2.33	226.77	90.67

Effect of Contact Time:

The effect of contact time on MB removal was studied over 0–60 min using UV–Visible spectrophotometry at 663–664 nm. Rapid removal was observed initially, reaching 97.6% at 25 min and 98.7% at 35 min, followed by gradual equilibrium at approximately 55 min. This behaviour is consistent with reported MB adsorption using porous and biomass-derived adsorbents [12–14]. The rapid initial uptake was attributed to abundant vacant surface sites, porous structure, and accessible functional groups, while progressive site occupation reduced the adsorption rate [12,13]. Overall, the composite showed rapid and efficient MB removal, with an optimum contact time of approximately 55 min.

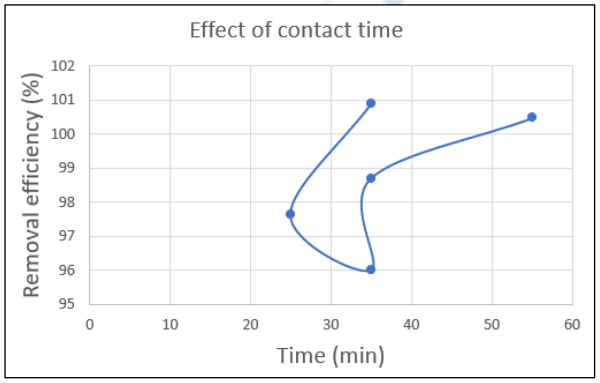


Fig. 5. Effect of Contact Time on Methylene Blue Removal Efficiency

Effect of Adsorbent Dosage:

- The effect of AC/CH/ZnO/PPy dosage on MB removal was studied over 5–25 mg. As shown in Fig. 6, removal efficiency varied with dosage, showing 100% at 5 mg, 98.7% at 10 mg, 96.0% at 15 mg, 97.6% at 20 mg, and 100% at 25 mg, with the highest apparent removal at 25 mg. Increasing adsorbent dosage generally provides more accessible adsorption sites and active surface area, enhancing MB uptake [17,18]. Amino and hydroxyl groups of chitosan may further contribute to dye interactions [19]. However, the observed non-monotonic trend may result from experimental variation, incomplete dispersion, particle aggregation, or optical interference from suspended particles. At higher dosages, aggregation and interparticle interactions may reduce effective surface-area accessibility [17,20]. Overall, 25 mg showed the highest apparent MB removal efficiency under the investigated conditions.

ISSN (Online) 2456 -1304

International Journal of Science, Engineering and Management (IJSEM)

Volume 13, Issue 9, September 2026

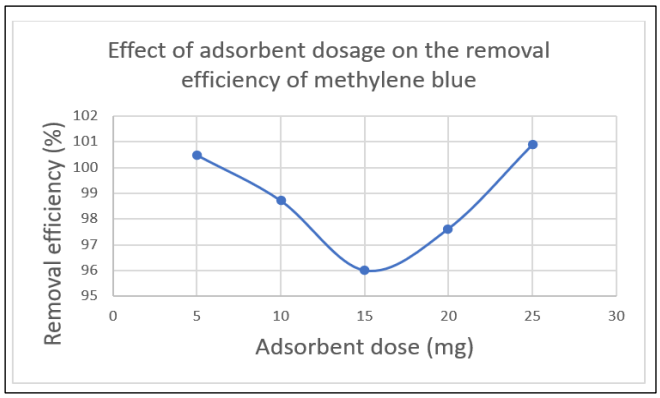


Fig. 6. Effect of Adsorbent Dose on Methylene Blue Removal Efficiency

Effect of Initial Dye Concentration:

The effects of initial MB concentration (25–175 mg/L) and contact time (0–55 min) were investigated. Rapid MB removal occurred initially, followed by slower uptake toward equilibrium, as commonly observed with porous and functionalized adsorbents [21–23]. At 25, 50, 75, and 100 mg/L, removal approached 100% within 15–30 min, whereas 150 and 175 mg/L required longer contact times, reaching 97.32% at 50 min and 98.03% at 45 min, respectively. Faster removal at lower concentrations was attributed to the greater availability of adsorption sites relative to MB molecules, while higher concentrations increased competition for active sites [22,23]. The rapid initial uptake was associated with abundant vacant sites, porous structure, and accessible surface functionalities of the composite [21,23]. Overall, near-complete MB removal was achieved within 15–30 min at lower initial concentrations under the investigated conditions.

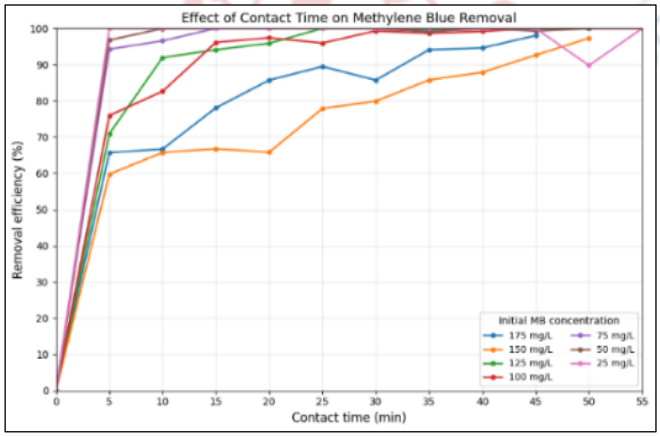


Fig. 7. Effect of contact time and initial methylene blue concentration on the removal efficiency of the AC/CH/ZnO/PPy bio-composite

C. Adsorption Kinetics:

The pseudo-first-order model showed moderate agreement with the experimental data (R^2 = 0.8419–0.9369) and underestimated q_e, indicating lower suitability for describing MB adsorption kinetics. In contrast, the pseudo-second-order model showed excellent agreement **(R^2 = 0.9688–0.9998),** with calculated q_e values closely matching the experimental values [25–27]. The k_2 value generally decreased with increasing initial MB concentration, indicating a lower apparent adsorption rate at higher dye concentrations [25,26]. Thus, the pseudo-second-order model provided the best kinetic fit. At 50 mg/L, the highest fit (R^2 = 0.9998) was obtained, with calculated and experimental q_e values of 50.00 and 51.74 mg/g, respectively [25,27]. However, the highest experimental q_e (171.56 mg/g) occurred at 175 mg/L, likely due to the greater concentration gradient and enhanced mass-transfer driving force, which promoted MB uptake [28,29].

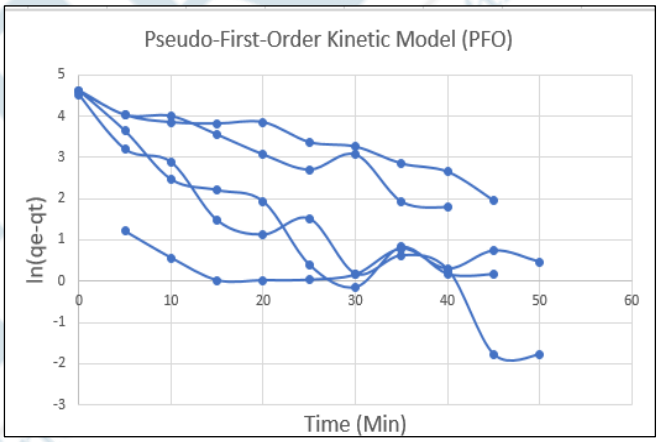


Fig. 8.a. Pseudo-First-Order Kinetic Model

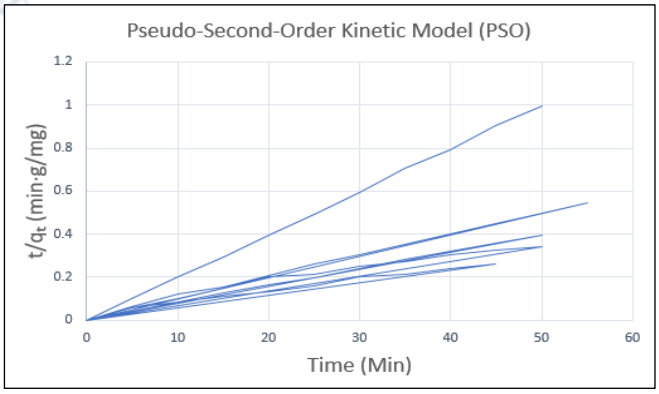


Fig. 8.b. Pseudo-Second-Order Kinetic Model

ISSN (Online) 2456 -1304

International Journal of Science, Engineering and Management (IJSEM)

Volume 13, Issue 9, September 2026

Table 2. Comparison Parameters of Pseudo-First Order and Pseudo-Second-Order Models (Ac/Ch/Zno/Ppy) On Methylene Blue Adsorption

Initial concentration (mg/L)	Experimental (q_e)	PFO (q_e)	PFO (R^2)	PSO (q_e)	PSO (R^2)	Best model
50	51.74	42.92	0.8616	50.00	0.9998	PSO
100	100.50	42.92	0.8616	102.04	0.9977	PSO
125	126.73	46.54	0.8419	129.87	0.9988	PSO
150	145.98	93.64	0.9279	149.25	0.9688	PSO
175	171.56	95.46	0.9369	175.44	0.9883	PSO

D. Antibacterial Activity:

The AC/CH/ZnO/PPy bio-composite showed antibacterial activity against both *E. coli* and *S. aureus*, with inhibition zones of 13 mm and 14 mm, respectively. The slightly higher activity against *S. aureus* may be related to differences in bacterial cell-envelope architecture; *S. aureus* has a thick peptidoglycan layer, whereas *E. coli* possesses a thinner peptidoglycan layer and an additional lipopolysaccharide-containing outer membrane [30,31]. ZnO nanoparticles may contribute through ROS generation, membrane disruption, oxidative damage, and Zn^{2+} release [32–34]. Chitosan further enhances antibacterial activity through electrostatic interactions between protonated amino groups and negatively charged bacterial surfaces, disrupting membrane integrity and promoting cellular leakage [35]. The porous activated-carbon and polypyrrole matrix may facilitate close contact with bacterial cells. Overall, the combined effects of ZnO-associated oxidative stress, chitosan-mediated electrostatic interactions, and carbon–polymer surface characteristics contribute to the antibacterial performance of the composite.

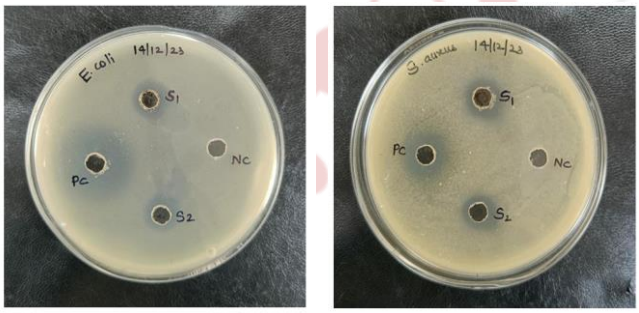


Fig. 9.A **Fig. 9.B**

Fig. 9. (A). Agar Well Diffusion with *E. coli*, (B). Agar Well Diffusion with *S. aureus*

E. Proposed Adsorption Mechanism:

The removal of methylene blue (MB) by the AC/CH/ZnO/PPy bio-composite can be attributed to surface interactions and diffusion through its porous structure. FTIR confirmed hydroxyl, amino, aromatic, and Zn–O functionalities, while SEM revealed a porous, heterogeneous surface providing accessible adsorption sites. Similar studies indicate that surface functional groups, pore structure, and accessible surface area collectively influence MB uptake [36–38]. The adsorption mechanism may involve electrostatic attraction, hydrogen bonding, π–π interactions, and pore diffusion [39–42]. Activated carbon provides the porous framework, chitosan supplies amino and hydroxyl groups, while ZnO and PPy enhance surface functionality. Thus, the high MB removal efficiency results from combined physical adsorption and specific surface interactions.

IV. CONCLUSION

The AC/CH/ZnO/PPy bio-composite demonstrated promising potential for methylene blue removal and antibacterial applications. Its porous structure and surface functional groups facilitated MB adsorption through electrostatic attraction, hydrogen bonding, π–π interactions, and pore diffusion. Adsorption kinetics were best described by the pseudo-second-order model, while pH 7.5 provided optimum removal efficiency (97.21%). The composite also exhibited antibacterial activity against *E. coli* and *S. aureus*, highlighting its multifunctional potential for wastewater treatment and antibacterial applications.

REFERENCES

[1] Lellis, B., Fávaro-Polonio, C. Z., Pamphile, J. A., & Polonio, J. C. (2019). Effects of textile dyes on health and the environment and bioremediation potential of living organisms. *Biotechnology Research and Innovation, 3*(2), 275–290. https://doi.org/10.1016/j.biori.2019.09.001

[2] Tkaczyk, A., Mitrowska, K., & Posyniak, A. (2020). Synthetic organic dyes as contaminants of the aquatic environment and their implications for ecosystems: A review. *Science of the Total Environment*, *717*, 137222. https://doi.org/10.1016/j.scitotenv.2020.137222

[3] Samsami, S., Mohamadizaniani, M., Sarrafzadeh, M.-H., Rene, E. R., & Firoozbahr, M. (2020). Recent advances in the treatment of dye-containing wastewater from textile industries: Overview and perspectives. *Process Safety and Environmental Protection, 143*, 138–163. https://doi.org/10.1016/j.psep.2020.05.034

[4] Hamad, N. N., & Idrus, S. (2022). Recent developments in the application of bio-waste-derived adsorbents for the removal of methylene blue from wastewater: A review. *Polymers*, *14*(4), 783. https://doi.org/10.3390/polym14040783

[5] Jin, Q., Li, Y., Yang, D., & Cui, J. (2018). Chitosan-derived

three-dimensional porous carbon for fast removal of methylene blue from wastewater. *RSC Advances, 8*, 1255–1264. https://doi.org/10.1039/C7RA11770A

[6] Abdi, Z., Bagheri, O., Kazemzadehhojaghan, M., & Malek Khachatourian, A. (2023). In situ synthesis of polypyrrole/Nd-doped ZnO nanocomposite with enhanced visible light photocatalytic performance for the degradation of organic dyes. *Materials Chemistry and Physics, 296*, 127248. https://doi.org/10.1016/j.matchemphys.2022.127248

[7] Ahmad, N., Sultana, S., Faisal, S. M., Ahmed, A., Sabir, S., & Khan, M. Z. (2019). Zinc oxide-decorated polypyrrole/ chitosan bionanocomposites with enhanced photocatalytic, antibacterial and anticancer performance. *RSC Advances, 9*, 41135–41150. https://doi.org/10.1039/C9RA06493A

[8] Mashkoor, F., & Nasar, A. (2020). Facile synthesis of polypyrrole decorated chitosan-based magsorbent: Characterizations, performance, and applications in removing cationic and anionic dyes from aqueous medium. *International Journal of Biological Macromolecules, 161*, 88–100. https://doi.org/10.1016/j.ijbiomac.2020.06.015

[9] Kohli, S., Nisha, Rathee, G., Hooda, S., & Chandra, R. (2023). Exploring the untapped catalytic application of a ZnO/CuI/PPy nanocomposite for the green synthesis of biologically active 2,4,5-trisubstituted imidazole scaffolds. *Nanoscale Advances, 5*, 2352–2360. https://doi.org/10.1039/D3NA00077J

[10] Maity, S. K., Tyagi, U., Sirohi, S., Pani, B., & Kumar, G. (2024). Fabrication of eco-friendly chitosan/polypyrrole composite for the removal of anionic dye from wastewater: Optimization and modeling studies. *Journal of Dispersion Science and Technology, 46*(1), 130–148. https://doi.org/10.1080/01932691.2023.2281519

[11] Huang, G., Chen, Z., Pan, Z., Xu, Y., Hu, H., & Wang, Y. (2023). Chemical dissolution-assisted ultrafine grinding for preparation of quasi-spherical colloids of zinc oxide. *Materials, 16*(7), 2558. https://doi.org/10.3390/ma16072558

[12] Wang, J., Tan, Y., Yang, H., Zhan, L., Sun, G., & Luo, L. (2023). On the adsorption characteristics and mechanism of methylene blue by ball mill modified biochar. *Scientific Reports, 13*, 21174. https://doi.org/10.1038/s41598-023-48373-1

[13] Ahmed, M. B., Zhou, J. L., Ngo, H. H., Guo, W., & Chen, M. (2023). Isotherm and kinetic investigations of sawdust-based biochar modified by ammonia to remove methylene blue from water. *Scientific Reports, 13*, 12772. https://doi.org/10.1038/s41598-023-39971-0

[14] Tang, X., Ran, G., Li, J., Zhang, Z., & Xiang, C. (2021). Extremely efficient and rapidly adsorb methylene blue using porous adsorbent prepared from waste paper: Kinetics and equilibrium studies. *Journal of Hazardous Materials, 402*, 123579. https://doi.org/10.1016/j.jhazmat.2020.123579

[15] Singh, R., & Edokpayi, J. N. (2020). Evaluation of methylene blue sorption onto low-cost biosorbents: Equilibrium, kinetics, and thermodynamics. *Journal of Chemistry, 2020*, 8318049. https://doi.org/10.1155/2020/8318049

[16] Ton, L. T., Pham, H.-D., Huynh, T.-N.-L., Duong, B.-N., et al. (2023). Adsorption of methylene blue from aqueous solution by biochar prepared from jackfruit peel: Isotherm model studies. *Vietnam Journal of Catalysis and Adsorption, 12*(1), 1–7. https://doi.org/10.51316/jca.2023.001

[17] Al-Tohamy, R., Ali, S. S., Li, F., Okasha, K. M., Mahmoud, Y. A.-G., Elsamahy, T., Jiao, H., Fu, Y., & Sun, J. (2022). A critical review on the treatment of dye-containing wastewater: Ecotoxicological and health concerns of textile dyes and possible remediation approaches for environmental safety. *Ecotoxicology and Environmental Safety, 231*, 113160. https://doi.org/10.1016/j.ecoenv.2021.113160

[18] Radoor, S., Karayil, J., Jayakumar, A., Parameswaranpillai, J., Lee, J., & Siengchin, S. (2022). Ecofriendly and low-cost bio adsorbent for efficient removal of methylene blue from aqueous solution. *Scientific Reports, 12*, 20580. https://doi.org/10.1038/s41598-022-22936-0

[19] Hosseini, S. M., Salari, M., & Naderi, M. (2021). Adsorption of methylene blue onto chitosan–montmorillonite/polyaniline nanocomposite. *Applied Clay Science, 203*, 105993. https://doi.org/10.1016/j.clay.2021.105993

[20] El Nemr, A., Abdelwahab, O., & El Sikaily, A. (2023). Olive stone as an eco-friendly bio-adsorbent for elimination of methylene blue dye from industrial wastewater. *Scientific Reports, 13*, 18791. https://doi.org/10.1038/s41598-023-47319-x

[21] Majamo, S. L., Amibo, T. A., & Mekonnen, D. T. (2024). Experimental investigation on adsorption of methylene blue dye from wastewater using corncob cellulose-based hydrogel. *Scientific Reports, 14*, 4540. https://doi.org/10.1038/s41598-024-54511-0

[22] Hidayat, E., Yonemura, S., Mitoma, Y., Harada, H., & Igwegbe, C. A. (2022). Methylene blue removal by chitosan cross-linked zeolite from aqueous solution and other ion effects: Isotherm, kinetic, and desorption studies. *Journal of Chemistry, 2022*, 1853758. https://doi.org/10.1155/2022/1853758

[23] Pourbaba, R., Abdulkhani, A., Rashidi, A., & Ashori, A. (2024). Lignin nanoparticles as a highly efficient adsorbent for the removal of methylene blue from aqueous media. *Scientific Reports, 14*, 9039. https://doi.org/10.1038/s41598-024-59612-4

[24] Abbasi, S., Nezafat, Z., Javanshir, S., & Aghabarari, B. (2024). Bionanocomposite MIL-100(Fe)/cellulose as a high-performance adsorbent for the adsorption of methylene blue. *Scientific Reports, 14*, 14497. https://doi.org/10.1038/s41598-024-65531-1

[25] Radoor, S., Karayil, J., Jayakumar, A., Parameswaranpillai, J., Lee, J., & Siengchin, S. (2023). Preparation and characterization of biopolymer-based adsorbents and their application for methylene blue removal from wastewater. *Scientific Reports, 13*, 15777. https://doi.org/10.1038/s41598-023-44613-6

[26] Wang, J., Tan, Y., Yang, H., Zhan, L., Sun, G., & Luo, L. (2023). On the adsorption characteristics and mechanism of methylene blue by ball mill modified biochar. *Scientific Reports, 13*, 21174. https://doi.org/10.1038/s41598-023-48373-1

[27] Khelifa, A., & Moulay, S. (2023). Removal of methylene blue by adsorption onto natural and purified clays: Kinetic and thermodynamic study. *MethodsX, 11*, 102393. https://doi.org/10.1016/j.mex.2023.102393

[28] Güneş, K. (2023). Isotherm and kinetic modeling of the adsorption of methylene blue, a cationic dye, on pumice. *International Journal of Chemistry and Technology, 7*(1), 1–9.

[29] Hidayat, E., Yonemura, S., Mitoma, Y., Harada, H., &

Igwegbe, C. A. (2022). Methylene blue removal by chitosan cross-linked zeolite from aqueous solution and other ion effects: Isotherm, kinetic, and desorption studies. *Journal of Chemistry, 2022*, 1853758. https://doi.org/10.1155/2022/1853758

[30] Silhavy, T. J., Kahne, D., & Walker, S. (2018). The bacterial cell envelope. *Cold Spring Harbor Perspectives in Biology, 10*(9), a000414. https://doi.org/10.1101/cshperspect.a000414

[31] Bhat, K. A., & Rather, M. A. (2021). Bacterial cell envelope and its role in antibacterial resistance. *Microbial Pathogenesis, 152*, 104665. https://doi.org/10.1016/j.micpath.2021.104665

[32] Sirelkhatim, A., Mahmud, S., Seeni, A., Kaus, N. H. M., Ann, L. C., Bakhori, S. K. M., Hasan, H., & Mohamad, D. (2015). Review on zinc oxide nanoparticles: Antibacterial activity and toxicity mechanism. *Nano-Micro Letters, 7*, 219–242. https://doi.org/10.1007/s40820-015-0040-x

[33] Zhang, R., Lee, Y.-C., & Lee, D.-H. (2020). ZnO nanomaterials: Current advancements in antibacterial mechanisms and applications. *Nanomaterials, 10*(7), 1274. https://doi.org/10.3390/nano10071274

[34] Sirelkhatim, A., Mahmud, S., Seeni, A., Kaus, N. H. M., Ann, L. C., Bakhori, S. K. M., Hasan, H., & Mohamad, D. (2015). Review on zinc oxide nanoparticles: Antibacterial activity and toxicity mechanism. *Nano-Micro Letters, 7*, 219–242. https://doi.org/10.1007/s40820-015-0040-x

[35] Younes, I., & Rinaudo, M. (2015). Chitin and chitosan preparation from marine sources: Structure, properties and applications. *Marine Drugs, 13*(3), 1133–1174. https://doi.org/10.3390/md13031133

[36] Cao, W., Wu, D., & Xiao, P. (2022). Synthesis of chitosan-glutaraldehyde/activated carbon composite for methylene blue adsorption: Optimization and mechanisms. *Desalination and Water Treatment, 270*, 275–288. https://doi.org/10.5004/dwt.2022.28793

[37] Liu, X.-J., Li, M.-F., Ma, J.-F., Bian, J., & Peng, F. (2022). Chitosan crosslinked composite based on corncob lignin biochar to adsorb methylene blue: Kinetics, isotherm, and thermodynamics. *Colloids and Surfaces A: Physicochemical and Engineering Aspects, 642*, 128621. https://doi.org/10.1016/j.colsurfa.2022.128621

[38] Dastoom, Z., et al. (2023). Production of $Ni_{0.5}Co_{0.5}Fe_2O_4$/activated carbon@chitosan magnetic nanobiocomposite as a novel adsorbent of methylene blue in aqueous solutions. *Scientific Reports, 13*, 6137. https://doi.org/10.1038/s41598-023-33470-y

[39] Nguyen, T. A., Juang, R.-S., & others. (2022). Synthesis of chitosan-glutaraldehyde/activated carbon composite for methylene blue adsorption: Optimization and mechanisms. *Desalination and Water Treatment, 270*, 275–288. https://doi.org/10.5004/dwt.2022.28793

[40] El Jery, A., Alawamleh, H. S. K., Sami, M. H., Abbas, H. A., Sammen, S. Sh., Ahsan, A., Imteaz, M. A., Shanableh, A., Shafiquzzaman, M., Osman, H., & Al-Ansari, N. (2024). Isotherms, kinetics and thermodynamic mechanism of methylene blue dye adsorption on synthesized activated carbon. *Scientific Reports, 14*, 970. https://doi.org/10.1038/s41598-023-50937-0

[41] Xue, H., et al. (2022). Adsorption of methylene blue from aqueous solution on activated carbons and composite prepared from an agricultural waste biomass: A comparative study by experimental and advanced modeling analysis. *Chemical Engineering Journal, 430*, 132801. https://doi.org/10.1016/j.cej.2021.132801

[42] El Nemr, A., Abdelwahab, O., & El Sikaily, A. (2023). Mechanistic insights into methylene blue removal via olive stone-activated carbon: A study on surface porosity and characterization. *Journal of Saudi Chemical Society, 27*, 101692. https://doi.org/10.1016/j.jscs.2023.101692